*ILASS–Europe 2022, 31st Conference on Liquid Atomization and Spray Systems, 6-8 September 2022, Virtual, Israel*

# CFD Simulations of Droplet Grouping in Acoustic Standing Waves

A. Arad*[1], V. Vaikuntanathan[2], M. Ibach[3],
J. B. Greenberg[4], B. Weigand[3], D. Katoshevski[1]
[1]Department of Civil and Environmental Engineering, Ben-Gurion University of the Negev (BGU), Beer-Sheva, Israel
[2]Department of Mechanical Engineering, Shiv Nadar University (SNU), UP, India
[3]Institute of Aerospace Thermodynamics (ITLR), University of Stuttgart, Stuttgart, Germany
[4]Aerospace Engineering, Technion–Israel Institute of Technology (IIT), Haifa, Israel
*Corresponding author: alumaha@post.bgu.ac.il

**Abstract**
In a previous study, acoustic waves were shown to have the potential to induce grouping of particles in exhaust systems [1]. In the present study, three-dimensional CFD simulations of single isopropanol droplet streams moving in air subjected to an acoustic field were performed with ANSYS Fluent. The Eulerian-Lagrangian approach was utilized based on the classical work of Gor'kov [2, 3] with the generalization of Settnes and Bruus [4]. The simulations reveal a grouping dynamics behavior of the droplets in acoustic standing waves (ASWs). The distances between the droplets in the stream are mainly affected by the droplet residence time which is the time a droplet spends in the ASW. The grouping dynamics also depend on the number of pressure nodes in the field.

**Keywords**
computational fluid dynamics (CFD), grouping, acoustic standing wave (ASW)

## Introduction

Numerical simulations of acoustic levitators are the subject of ongoing research [5] and are advantageous, especially when the acoustic levitator or the levitated particle has a complex geometry. In the present study, the geometry of the acoustic levitator and the droplet stream required 3D simulations, as shown below in Figure 1. In [5], an acoustic levitator was designed with a reflector radius of 20mm and a distance of approximately 30mm between the sonotrodes, with a transducer velocity amplitude of 1m/s. Previously, Reipschläger et al. [6] studied ultrasonic standing wave atomization using both experiments and numerical simulations. Because of different time scales and length scales, they decoupled the simulations into a first step of oscillating velocity and pressure in the ultrasonic field and a second step of 3D Direct Numerical Simulations (DNS) of the droplet disintegration process. Good qualitative agreement was obtained between the experiments and simulations with respect to the disintegration mechanism.

Recently, acoustic waves were shown to have the potential to induce grouping of particles in exhaust systems [1]. A phenomenological 1D model was used to analyze the process and shed light on the effects of the sound waves and flow oscillations on particle trajectories in the acoustic field. In the present study, we studied the dynamics of isopropanol droplets surrounded by air in an acoustic levitator using both CFD simulations and experiments. A scheme of the experimental system is shown in Figure 1, and an image of the experimental results is shown in Figure 2. Droplet grouping was obtained in the experiments. Descriptions of the experiments used to validate the present CFD simulations are provided in Vaikuntanathan et al. [7].

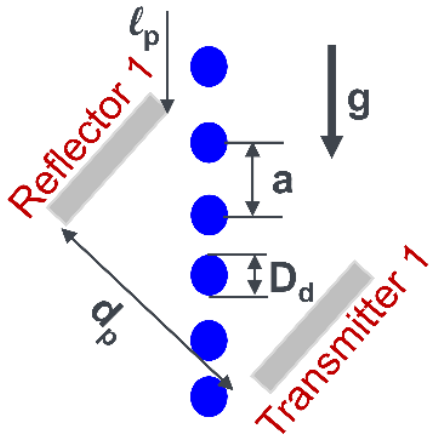


*Figure 1: The acoustic levitator system with droplets moving between the sonotrodes. The dimensionless interdroplet distance is $a/D_d$. $d_p$ =* 26mm, and the sonotrode radius is 20mm.

*Figure 2: Magnified image of acoustic-induced grouping in the experiments at ITLR, 7ms after the switching on of the acoustic field, showing a combination of single droplets and droplet pairs.*

**Computational approach and modeling considerations**

CFD simulations were performed using the Eulerian-Lagrangian approach. The continuous phase here is air. The following conservation equations were solved for the continuous phase: mass, momentum, and energy, together with the ideal gas equation of state. For the discrete phase (which is composed of the liquid droplets), a force balance was solved.

The acoustic force on a compressible particle in an acoustic standing wave (ASW) was modeled in the classic work of Gor'kov [2]. Iorio and Perfetti [3] employed this theory to study the acoustic field of flows in channels.

The acoustic force formulation on a spherical particle proposed by Gor'kov [2] is based on the acoustic potential <*U*>:

$$\langle U \rangle = \frac{4}{3}\pi R_p^{\,3}\left( f_1 \langle E_{pot} \rangle - \frac{3}{2} f_2 \langle E_{kin} \rangle \right). \qquad (1)$$

Here, $\langle E_{pot} \rangle$ is the time-averaged potential energy, $\langle E_{kin} \rangle$ is the time-averaged kinetic energy, $f_1$ and $f_2$ are the material contrast factors, and $R_p$ is the particle radius.

The time-averaged potential energy is given by:

$$\langle E_{pot} \rangle = \frac{\langle p^2 \rangle}{2\rho_m c_m^{\,2}}, \qquad (2)$$

where $p$ is the transient local pressure in the gas phase, $\rho_m$ is the medium density, and $c_m$ is the sound velocity in the medium.

The time-averaged kinetic energy is given by:

$$\langle E_{kin} \rangle = \rho_m \langle v^2 \rangle / 2 \qquad (3)$$

where $v$ is the transient local velocity in the gas phase.

The material contrast factors $f_1$ and $f_2$ are given by:

$$f_1 = 1 - \left(\rho_m c_m^2\right) / \left(\rho_p c_p^2\right) \tag{4}$$

and

$$f_2 = \frac{2\left(\rho_p - \rho_m\right)}{2\rho_p + \rho_m}, \tag{5}$$

where $\rho_p$ is the particle density, and $c_p$ is the sound velocity in the particle.

Finally, the force $\vec{F}_{ASW,G}$ on the particle is the gradient of the acoustic potential:

$$\vec{F}_{ASW,G} = -\nabla \langle U \rangle . \tag{6}$$

The acoustic potential of Gor'kov was generalized by Settnes and Bruus [4] with a different contrast factor $f_2$:

$$f_2 = \mathrm{Re}\left[\frac{2\left[1-\gamma\left(\tilde{\delta}\right)\right](\tilde{\rho}-1)}{2\tilde{\rho}+1-3\gamma\left(\tilde{\delta}\right)}\right], \tag{7}$$

where $\gamma\left(\tilde{\delta}\right)$ is a complex valued viscosity coefficient which depends on $\tilde{\delta}$:

$$\gamma\left(\tilde{\delta}\right) = -\frac{3}{2}\left[1+i\left(1+\tilde{\delta}\right)\right]\tilde{\delta}, \tag{8}$$

$\tilde{\delta}$ is the dimensionless acoustic boundary layer thickness:

$$\tilde{\delta} = \frac{\sqrt{2\nu/\omega}}{R_p} \tag{9}$$

with the medium kinematic viscosity v and acoustic field angular frequency ω, and $\tilde{\rho}$ is the density ratio:

$$\tilde{\rho} = \rho_p / \rho_m . \tag{10}$$

The acoustic field properties were calculated following Lessmann [8]. The acoustic potential and the force on a droplet in the ASW were incorporated into ANSYS Fluent using User Defined Functions (UDFs) and calculated and saved as User Defined Memory (UDM).

**Results and discussion**

Figures 3–6 show variables of the acoustic field for three cases: one, two, and three pressure nodes. In these figures, a section of the cylindrical domain is shown in the xz plane. The droplets move in the -z direction, which is shown by a purple arrow in Figure 3. The location of the sonotrodes, which have a shape of a disc, is shown in Figure 3. The outlet has a shape of a cylindrical shell. Figure 3 shows the time-averaged acoustic potential energy calculated by Equation 2. Figure 4 shows the time-averaged acoustic kinetic energy calculated by Equation 3. Figure 5 shows the acoustic potential calculated by Equation 1. Figure 6 shows the acoustic force calculated by Equation 6. Finally, Figure 7 shows the dimensionless distance between consecutive droplets of a stream in an ASW with three pressure nodes.

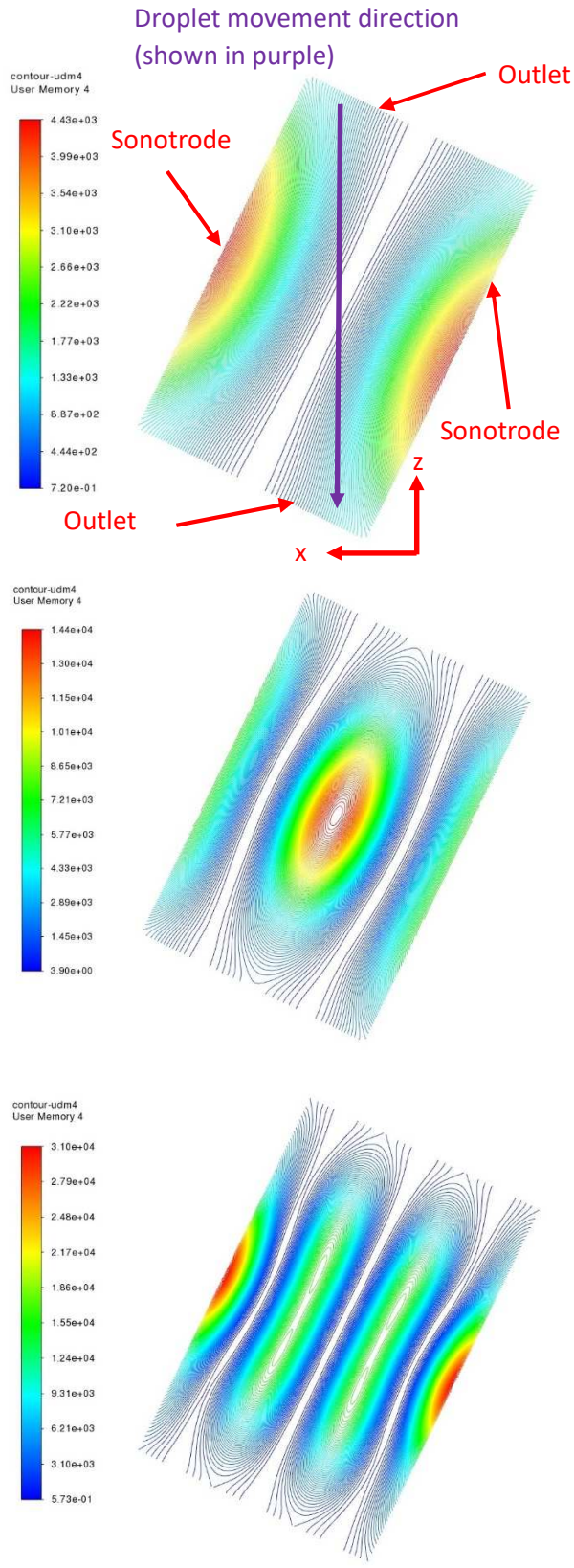


*Figure 3: Time-averaged acoustic potential energy [J/m$^3$] in different ASWs: top, one node; middle, two nodes; bottom, three nodes.*

This figure and the following ones show the calculated variables in the section of the cylindrical computational domain with the following directions: the sonotrodes at northwest and southeast, and the outlet at northeast and southwest.

In Figure 3, the pressure nodes are seen where the acoustic potential energy is minimal. These are the locations where the pressure itself is approximately zero. The maximal acoustic potential energy increases with the number of pressure nodes. Generally, the acoustic potential energy in each case is symmetrical across the midline of the computational domain section.

The zones with larger potential energy are zones where the acoustic potential is increased since the potential energy is preceded by a plus sign in the equation for the acoustic potential (Equation 1).

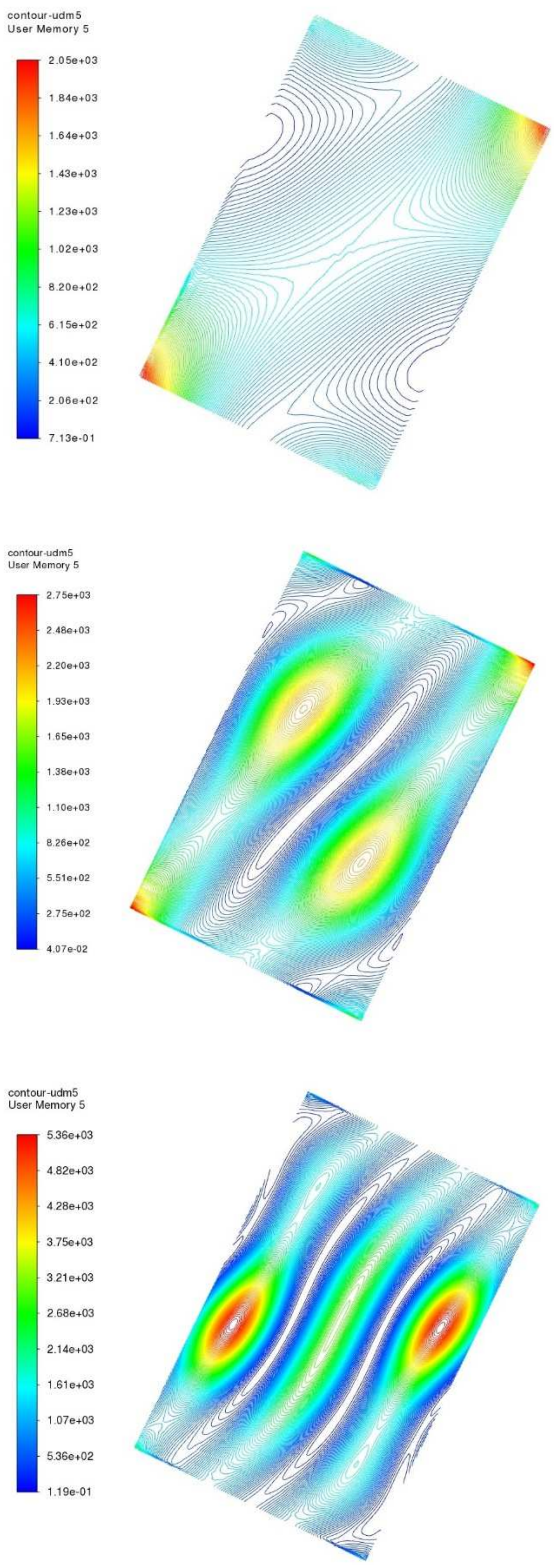


*Figure 4: Time-averaged acoustic kinetic energy [J/m$^3$] in different ASWs: top, one node; middle, two nodes; bottom, three nodes.*

In Figure 4, the time-averaged kinetic energy is not symmetric across the midline of the computational domain section in all three cases. The velocity before initiation of the acoustics levitator is zero in the computational domain. Thus, the velocity field is induced only by the acoustic levitator. There are some similarities between the three cases. First, with one pressure node and two pressure nodes, the maximal values are obtained at the top right and bottom left-hand corners. Second, closed contours are obtained in the computational domain with two and three pressure nodes. The zones with larger kinetic energy are zones where the acoustic potential is reduced since the kinetic energy is subtracted from the potential energy in the equation for the acoustic potential (Equation 1).

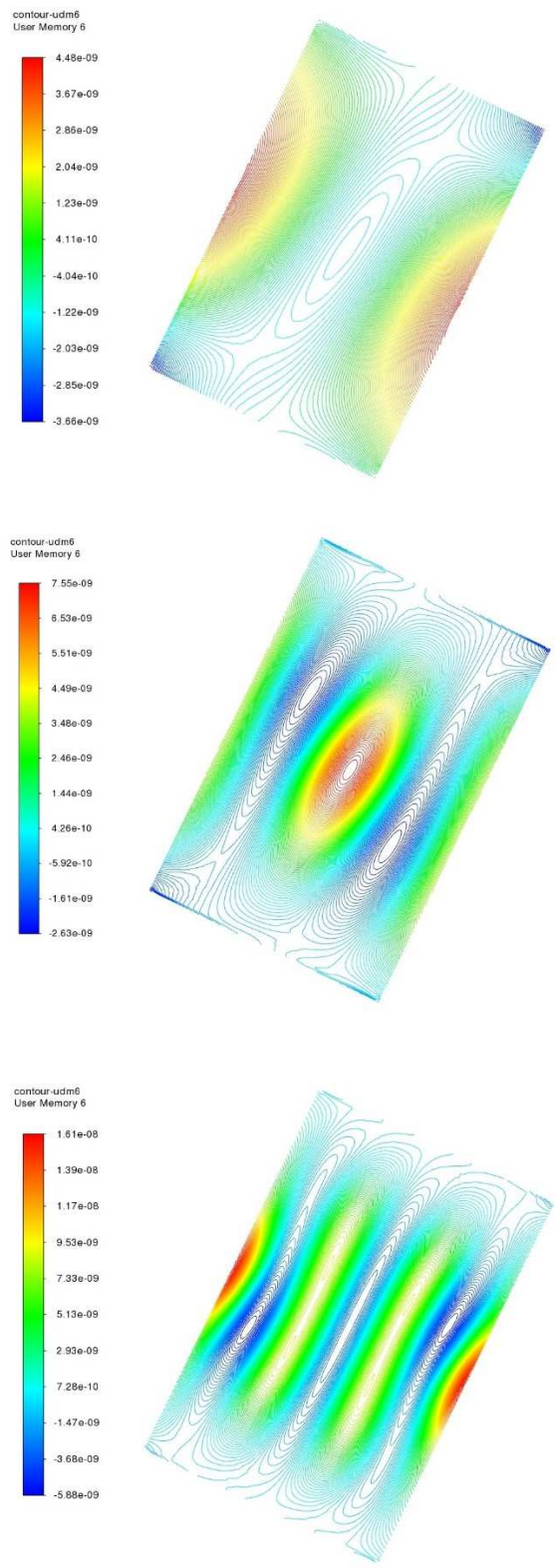


*Figure 5: Acoustic potential in different ASWs [J]: top, one node; middle, two nodes; bottom, three nodes.*

The acoustic potential can be regarded as a superposition of the time-averaged kinetic and potential energies [3]. It is given by Equation 1. In this equation, the time-averaged potential energy and the time-averaged kinetic energy are multiplied by the material contrast factors $f_1$ and $f_2$, respectively. In addition, the time-averaged kinetic energy is multiplied by a coefficient of 1.5. The time-averaged kinetic energy is lower than the time-averaged potential energy. However, $f_1$ is approximately unity, whereas $f_2$ is equal to 1.63, 1.57, and 1.46, for one node, two nodes, and three nodes, respectively. Although the time-averaged kinetic energy is lower than the time-averaged potential energy, due to these coefficients the time-averaged kinetic energy reduces the acoustic potential significantly, such that its effect on the acoustic potential is seen in Figure 5. Specifically, the deviation from symmetry is apparent in all three cases examined here.

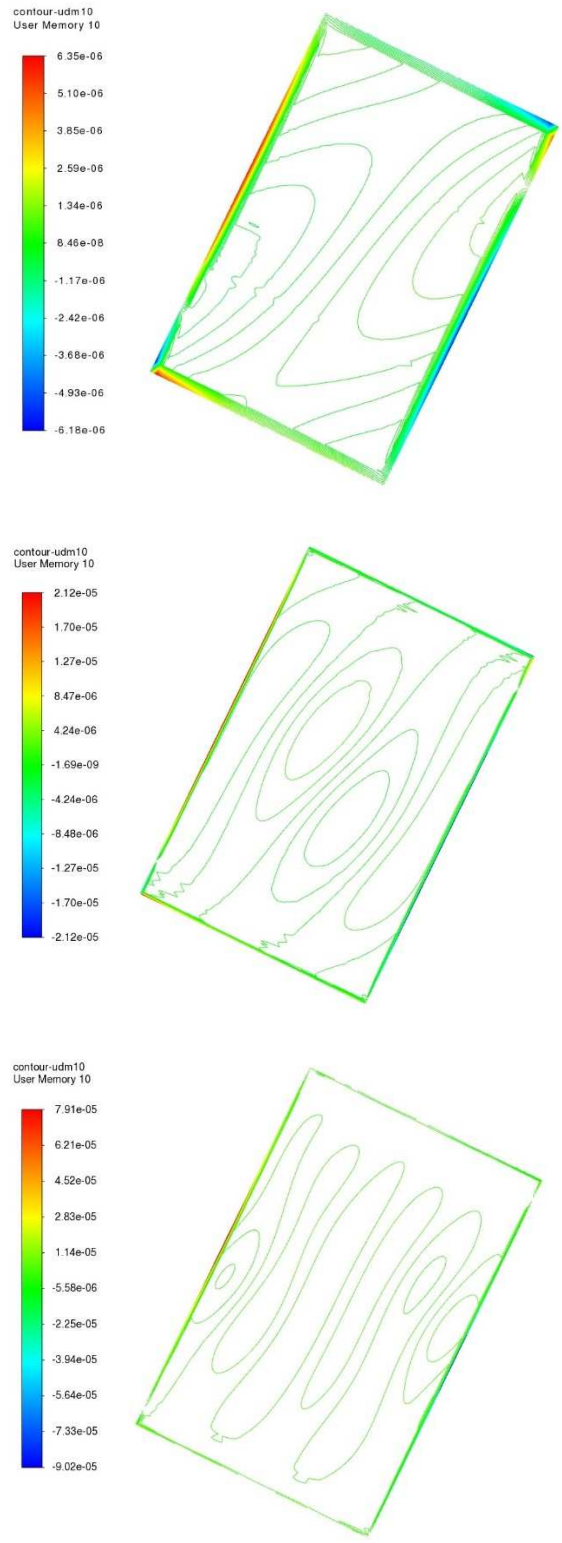


*Figure 6: Force on the particle [N] in the gravitational direction in ASWs: top, one node; middle, two nodes; bottom, three nodes.*

Figure 6 shows the force component in the gravitational direction for three cases: one node, two nodes, and three nodes. The contours of the force are significantly different in these cases in both magnitude and shape. For example, with one node, there are no closed contours, whereas with two and three nodes, there are closed contours, yet at different locations. With two nodes, the closed contours are larger and closer to the center of the computational domain. Therefore, grouping in a stream of droplets in each of these force distributions is different. Moreover, grouping depends on the location of injection in each of these force distributions. Different injection points in each distribution lead to different grouping times. Thus, varying grouping behavior can be achieved by changing the number of pressure nodes or even the location of the injection with each number of pressure nodes.

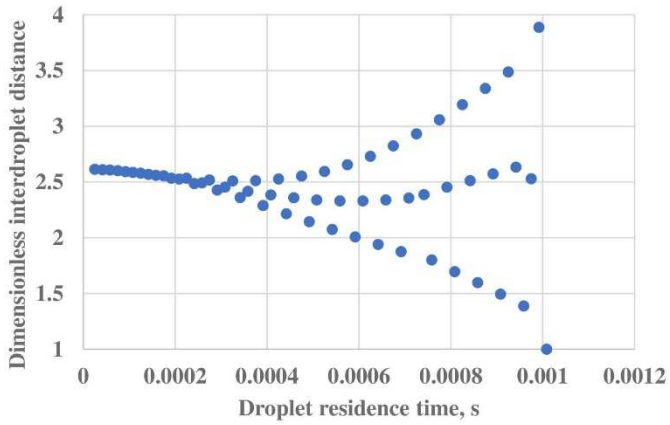


*Figure 7: Dimensionless distance $a/D_d$ between consecutive droplets of a stream in an ASW with three pressure nodes.*

In Figure 7, which shows the dimensionless distance between consecutive droplets, smaller distances indicate pairs of droplets, whereas larger ones show the distinct distances between pairs. The sequence of consecutive small distances, intermediate distances, and large distances shows a droplet pair and a single droplet, similarly to the experimental results, which showed a combination of single droplets and droplet pairs in the droplet stream in the ASW (see Figure 2).

## Conclusions

Grouping in droplet streams in ASWs was studied in a 3D system using both CFD simulations and experiments. In the CFD simulations, grouping was found to depend on the number of pressure nodes in the acoustic field and the injection location in the ASW. With three pressure nodes, a combination of droplet pairs and single droplets was obtained, similarly to the experimental results. Using the acoustic levitator, the grouping behavior can be varied by changing the number of pressure nodes or even the location of the injection with each number of pressure nodes.

## Acknowledgments

This study was conducted with the financial support of the Deutsche Forschungsgemeinschaft (DFG, German Research Foundation) through the project 'Investigation of Droplet Motion and Grouping' (project number 409029509). It was also funded by DFG under Germany's Excellence Strategy - EXC 2075 – 390740016. We also acknowledge the support of the Stuttgart Center for Simulation Science (SimTech). We also acknowledge the financial support of the Israeli Ministry of Science, Technology and Space, grant # 3-16515.

The authors would like to thank Dr. Eduard Moses for his assistance with the ANSYS Fluent software.

## References

[1] Zhang Z., Abom M., Boden H., Karlsson M., Katoshevski D., 2017. *SAE International Journal of Engines* 10 (4).
[2] Gor'kov, 1962. Translation to English. *Soviet Physics – Doklady* 6(9), 315–317.
[3] Iorio C. S., Perfetti, C., 2015. *Fluid Dynamics and Material Processing* 11 (1), 27–48.
[4] Settnes and Bruus, 2012. *Physical Review E* 85, 016327 (1–12).
[5] Zhang D., 2020. "Acoustic levitation, from physics to applications", Springer.
[6] Reipschläger O., Bothe D., Warnecke H. J., Monien B., Prüss J., Weigand B., 2002. ILASS Europe 2002, Zaragoza 9–11 September.
[7] Vaikuntanathan V., Amini K., Arad A., Katoshevski D., Greenberg B., & Weigand B., 2021. ICLASS 2021, 15th Triennial International Conference on Liquid Atomization and Spray Systems, Edinburgh, UK, 29 August–2 September.
[8] Lessmann N. 2004. Numerical and experimental investigation of the disintegration of polymer melts in an ultrasonic standing wave atomizer. Doctoral Dissertation, University of Paderborn.